Distinct Activation States of α5β1 Integrin Show Differential Binding to RGD and Synergy Domains of Fibronectin†

Andrés J. García,*,‡ Jean E. Schwarzbauer,§ and David Boettiger‡

Department of Microbiology, University of Pennsylvania, Philadelphia, Pennsylvania 19104, and Department of Molecular Biology, Princeton University, Princeton, New Jersey 08544

Received March 1, 2002; Revised Manuscript Received May 10, 2002

ABSTRACT: α5β1 integrin can occupy several distinct conformational states which support different strengths of binding to fibronectin [García, A. J., et al. (1998) *J. Biol. Chem. 273*, 34710−34715]. Using a model system in which specific activating monoclonal antibodies were used to achieve uniform activated states, the binding of α5β1 to full-length wild-type fibronectin and mutants of fibronectin in the defined RGD and PHSRN synergy sites was analyzed using a novel method that measures the strength of the coupling between integrin and its ligand. Neither TS2/16- nor AG89-activated α5β1 showed significant mechanical coupling to RGD-deleted fibronectin. However, peptide competition assays demonstrated a 6-fold difference in the binding affinities of these two states for RGD. The mutant synergy site reduced the AG89 (low)-activated state to background levels, but the TS2/16-activated state still retained approximately 30% of the wild-type activity. Thus, these two active binding states of α5β1 interact differently with both the RGD and synergy domains. The failure of the AG89-activated state to show mechanical coupling to either the RGD or synergy domain mutants was unexpected and implies that the RGD domain itself does not contribute significant mechanical strength to the α5β1−fibronectin interaction. The lack of RGD alone to support α5β1 coupling was further confirmed using a synthetic polymer presenting multiple copies of the RGD loop. These results suggest a model in which the RGD domain serves to activate and align the α5β1−fibronectin interface, and the synergy site provides the mechanical strength to the bond.

The binding of integrin adhesion receptors to their extracellular ligands plays a central role in development and inflammation (*1*, *2*), and abnormalities in integrin binding have been associated with many pathological conditions such as cancer metastasis and blood clotting defects (*3*). Affinity modulation or "inside-out signaling" provides a rapid and reversible mechanism for control of integrin−ligand interactions (*4*). Modulation of binding affinity has been shown to regulate numerous adhesion events, including platelet aggregation (*5*), fibronectin matrix assembly (*6*, *7*), and epithelial and myogenic differentiation (*8*, *9*).

Affinity modulation involves conformational changes in the integrin receptor (*10*), and shifts between inactive and active binding states can be detected by changes in antibody binding (*11*), changes in the strength of the integrin−ligand bond (*12*), or fluorescence resonance energy transfer (*13*). Although the mechanistic basis by which the cell controls the switching of integrin conformations remains unclear, several molecules, including the CD98 T-cell activation antigen (*14*) and members of the Ras family of GTP-binding proteins (*15*, *16*), have been implicated in the activation process. In addition to intracellular signaling events, integrins can be activated by divalent cations and integrin-specific monoclonal antibodies (*17*−*20*). These extrinsic reagents provide a simple and uniform means of manipulating integrin activation to analyze the functional binding states of these receptors.

Using a novel mechanical approach to analyze the integrin−fibronectin bond, we previously showed the existence of three distinct activation states for α5β1 integrin that produced distinct strengths of binding to fibronectin (*12*). Since these distinct functional binding states are likely to arise from interactions of α5β1 integrin with different sites in fibronectin, in this study we analyzed the strength of binding of activated forms of α5β1 to full-length recombinant fibronectins which contained mutations in defined α5β1 integrin binding sites. Integrin α5β1 binds cooperatively to the RGD site in the 10th type III repeat and the PHSRN sequence in the 9th type III repeat of fibronectin (*21*−*23*). The requirement for the PHSRN synergy site in α5β1-mediated adhesion to fibronectin appears to depend on the activation state of the integrin. Danen et al. demonstrated that activation of α5β1 to a high-affinity state via stimulatory antibodies reduced the need for the PHSRN site in cell adhesion (*23*). Similarly, activation of α5β1 by extrinsic factors reduced the requirement of the PHSRN site for fibronectin matrix assembly (*7*). These studies support a model in which PHSRN stabilizes the binding of α5β1 to

† Financial support of the National Institutes of Health through Contracts CA-16502, CA-49866, and GM-57388.

* To whom correspondence should be addressed: Woodruff School of Mechanical Engineering and Petit Institute for Bioengineering and Bioscience, Georgia Institute of Technology, 315 Ferst Dr., 2314 IBB, Atlanta, GA 30332-0363. E-mail: andres.garcia@me.gatech.edu. Phone: (404) 894-9384. Fax: (404) 385-1397.

‡ University of Pennsylvania.

§ Princeton University.

10.1021/bi025752f CCC: $22.00
Published on Web 06/26/2002

RGD, and these contributions from the PHSRN site are no longer necessary when the integrin is in its high-affinity state. Contrary to this simple paradigm, the analysis presented here demonstrates that the RGD site by itself does not support measurable mechanical coupling to $\alpha5\beta1$, even when the integrin is in its high-affinity state. More importantly, our results support a dynamic binding process in which different conformations of $\alpha5\beta1$ interact with different binding surfaces on fibronectin, including but not limited to the RGD and PHSRN sites, to produce distinct functional binding strengths. This dynamic model could provide an explanation for the diverse signaling responses that originate from this receptor−ligand interaction (*24*, *25*).

EXPERIMENTAL PROCEDURES

Cells and Recombinant Fibronectins. Human K562 erythroleukemia cells were grown in Dulbecco's modified Eagle's medium supplemented with 10% calf serum and 1% penicillin-streptomycin. During growth, K562 cells were selected for growth in suspension as single cells, which results in the absence of detectable specific adhesion to fibronectin. Monoclonal antibodies TS2/16 (ATCC), AG89 (kindly donated by J. Takagi, Harvard Medical School, Boston, MA), and BIIG2 (kindly provided by C. H. Damsky, University of California, San Francisco, CA) were affinity purified from hybridoma supernatants on protein G−Sepharose columns. Other reagents were obtained from Life Technologies (Gaithersburg, MD).

The pVL1392 baculovirus vector was used for expression of all recombinant fibronectins. Full-length rat fibronectin cDNA constructs for wild-type and mutant fibronectins have been described previously (*7*, *26*). The RGD mutant [FN-(RGD−)][1] is a deletion of these three amino acids; the synergy site mutant [FN(syn−)] changes the PPSRN sequence to PGSEN (rat sequence equivalent to the human PHSRN site). Proteins were expressed in baculovirus-infected insect cells (BTI-TN-5B-4, Invitrogen, San Diego, CA) and purified by gelatin−agarose affinity chromatography (*26*).

Cell Adhesion Assay. Cell adhesion was quantified using a spinning disk device as described previously (*12*, *27*). This system applies a well-defined range of hydrodynamic forces to cells adhering to fibronectin-coated circular coverslips. The applied shear stress τ (force per area) increases linearly with radial position r along the coverslip surface and is given by

$$\tau = 0.8r\sqrt{\rho\mu\omega^3}$$

where ρ and μ are the fluid density and viscosity, respectively, and ω is the rotational speed. Glass coverslips (25 mm in diameter) were coated with recombinant fibronectins (5 μg/mL) for 30 min and blocked in 1% bovine serum albumin for 30 min. K562 cells were resuspended in Dulbecco's phosphate-buffered saline with 2 mM glucose in the presence of saturating amounts of stimulatory or inhibitory antibodies. Cells were seeded onto fibronectin-coated substrates for 15 min and spun at a constant speed for 10 min. For inhibition experiments, cells were seeded in the presence of varying concentrations of RGDS peptide. After being spun, adherent cells were fixed in 3.7% formaldehyde and 1% Triton X-100 and stained with ethidium homodimer. Using an automated motorized stage and image analysis system, nuclei were counted at different radial positions and normalized to the counts at the disk center for which the applied force is zero. The resulting detachment profile (adherent fraction f vs applied shear stress τ) was fitted to a sigmoid curve $f = 1/\{1 + \exp[b(\tau - \tau_{50})]\}$, where τ_{50} is the shear stress for 50% detachment and b is the inflection slope (*27*).

[1] Abbreviations: wtFN, wild-type fibronectin; FN(RGD−), fibronectin mutant lacking the RGD binding site; FN(syn−), fibronectin with a mutated synergy site.

RESULTS

Assessment of Mechanical Coupling between $\alpha5\beta1$ Integrin and Fibronectin. In contrast to conventional cell adhesion and spreading assays, we focus on the initial (15 min) interaction between $\alpha5\beta1$ and fibronectin using an ultrasensitive cell adhesion assay. Our hydrodynamic flow system applies a well-defined range of forces to adherent cells and provides direct measurements of cell adhesion strength (*27*). A critical aspect of this quantitative assay is the use of K562 erythroleukemia cells as a model cell system. These cells express $\alpha5\beta1$ as the only fibronectin receptor, and this integrin is expressed in a constitutively inactive form which can be activated with monoclonal antibodies or divalent cations (*28*, *29*). More importantly, under the experimental conditions of the assay, these cells do not exhibit adhesion strengthening, and there are no differences in adhesion strength between 5 and 15 min or at 15 min in the presence of metabolic poisons, allowing the isolation of the initial receptor−ligand interaction from subsequent stages of the adhesion process, including cytoskeletal interactions (*27*). We previously demonstrated that, for equivalent cell populations and ligand densities, differences in the detachment force reflect differences in the mechanical strength of the integrin−fibronectin bond (*27*). Therefore, this system provides sensitive, direct measurements of the strength of the $\alpha5\beta1$−fibronectin interaction in intact cells.

Figure 1A is a typical cell detachment profile showing the fraction of adherent cells as a function of shear stress (applied force per area) for the adhesion of TS2/16-activated K562 cells to recombinant rat fibronectin. The sigmoid curve follows the expected relationship for a cell population with a normally distributed receptor density. The shear stress for 50% detachment (τ_{50}) represents the mean cell adhesion strength. This analysis is based on the measurement of 10000−20000 cells, providing robust statistics. The mean cell adhesion strength is a direct measurement of the mechanical coupling between $\alpha5\beta1$ and fibronectin.

Since the number of receptor−ligand bonds, and consequently adhesion strength, is dependent on ligand density, the adsorption profiles of the three recombinant fibronectins were compared using an ELISA-based assay to account for differences in adsorption. Figure 1B shows no differences in adsorbed densities among the recombinant proteins. To ensure that the recombinant fibronectin behaved like fibronectin isolated from plasma, the two were compared by measuring the adhesion strength as shown in Figure 1A. Specific activating antibodies (AG89 and TS2/16) were used at saturating concentrations to achieve uniform activation of $\alpha5\beta1$ on K562 cells. We have shown that, for the same

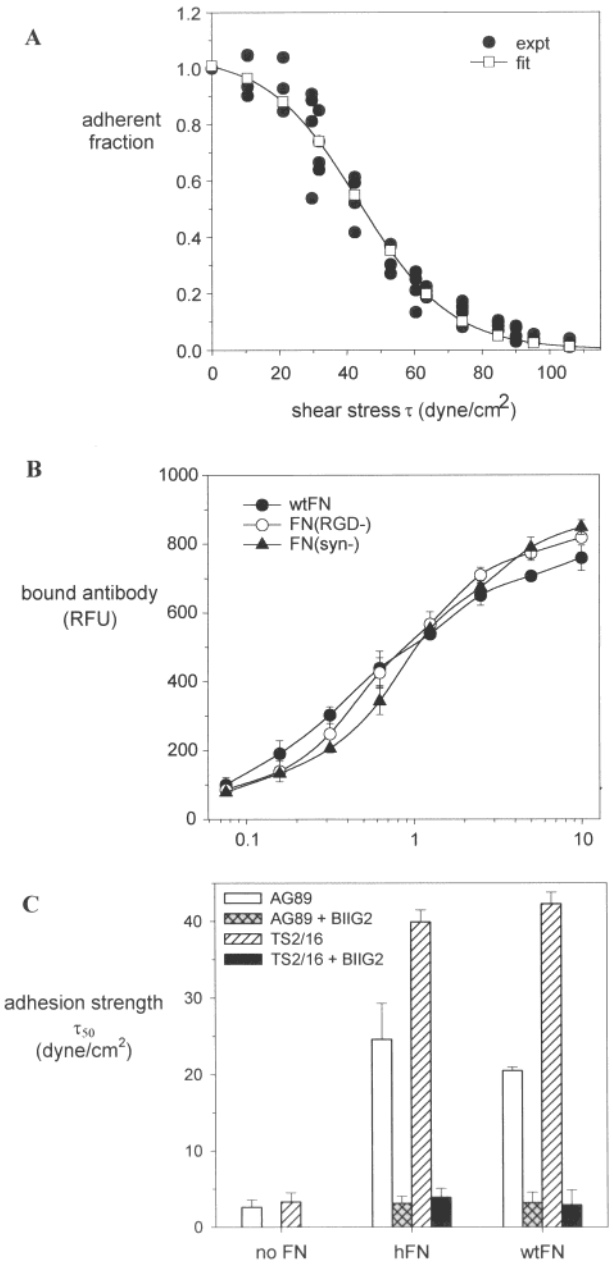

FIGURE 1: Strength of adhesion to recombinant wild-type fibronectin. (A) Cell detachment profile of TS2/16-activated K562 cells binding to recombinant rat fibronectin showing the fraction of adherent cells (f) as a function of applied surface shear stress (τ). This profile was fitted to a sigmoid curve to obtain the shear stress for 50% detachment (τ_{50}) which represents the mean cell adhesion strength. (B) Adsorption profiles for recombinant rat fibronectins showing no differences in adsorption behavior among recombinant proteins. Proteins were adsorbed onto tissue culture polystyrene and analyzed by ELISA using a monoclonal antibody against the heparin-binding domain of rat fibronectin. Values represent the mean and standard error of three measurements. (C) AG89 and TS2/16 antibody-activated adhesion of K562 cells to recombinant rat wild-type fibronectin (wtFN) is equivalent to adhesion to human plasma fibronectin (hFN). Cells were plated on substrates coated with 5 μg/mL wtFN or hFN, and adhesion was quantified using the spinning disk device. Adhesion was completely blocked by the anti-α5 antibody (BIIG2) that inhibits binding to fibronectin.

number of activated integrins, these antibodies produce different activation states characterized by different strengths of binding to adsorbed human plasma fibronectin (*12*). These differences in binding strength between the two activation conditions do not arise from differences in binding affinity as these two activated states exhibit equivalent binding affinities (1.1×10^7 M^{-1}) for soluble fibronectin (*12*). This analysis indicated that these different functional binding strengths reflect different strengths of the integrin−fibronectin interaction. Stimulation with AG89 was indistinguishable from integrin activation with 1.0 mM Mn^{2+}, indicating that these activation conditions are functionally equivalent (*12*). Figure 1C shows that both plasma fibronectin and recombinant wild-type fibronectin exhibited a 2-fold difference between the TS2/16- and AG89-activated states of α5β1 integrin. In addition, the extent of adhesion for both activated states was reduced to background levels by preincubation with the α5 integrin blocking monoclonal antibody BIIG2. These results show equivalent functional binding between human plasma fibronectin and recombinant rat fibronectin, indicating that small differences in amino acid sequence between these two species do not significantly influence functional integrin binding.

A likely explanation for the functional differences in binding strengths for the two activated states is that these states represent distinct conformations of the receptor that interact differently with binding domains in fibronectin. On the basis of the conventional model of α5β1 binding to fibronectin involving both RGD and PHSRN synergy domains, we postulated that the lower activation state (equivalent to AG89 stimulation) primarily entails binding to the RGD domain and that the higher-activity state (corresponding to TS2/16 stimulation) involves binding to both RGD and PHSRN synergy domains. This hypothesis was tested using the two activated states of α5β1 and the three recombinant fibronectins.

Interaction of α5β1-Activated States with the RGD Domain. The adhesion strength for binding of antibody-activated integrins to wild-type fibronectin (wtFN) or the RGD mutant [FN(RGD−)] was measured. Figure 2 shows that deletion of the RGD domain reduced the strength of α5β1-mediated adhesion to background levels for both TS2/16- and AG89-activated forms. This result is not surprising given the central role established for RGD in the binding of α5β1 to fibronectin (*21*, *30*, *31*). However, the spinning disk method applied here is more sensitive than previous approaches and has been able to identify weak adhesion states which were not observed using earlier methods (*32*). Thus, these results extend the resolution of the analysis and demonstrate that all other domains of fibronectin are unable to mediate any significant adhesion in the absence of the RGD site. These data contrast with the observations of Koteliansky that many fibronectin type III repeats could mediate adhesion in a manner independent of the RGD site (*33*).

To analyze the ability of RGD to bind to the two activated states of α5β1 integrin, soluble RGDS peptide was used as a competitive inhibitor of TS2/16- and AG89-activated α5β1-mediated adhesion to wild-type fibronectin. Figure 3 shows the normalized mean adhesion strength for experiments run in the presence of different concentrations of RGDS peptide. The affinity of the AG89-activated α5β1 for RGDS peptide was 6-fold higher than that for TS2/16-activated α5β1. This difference indicates that these two active states of α5β1 interact differently with RGD peptides and hence may interact differentially with the RGD loop in the 10th type

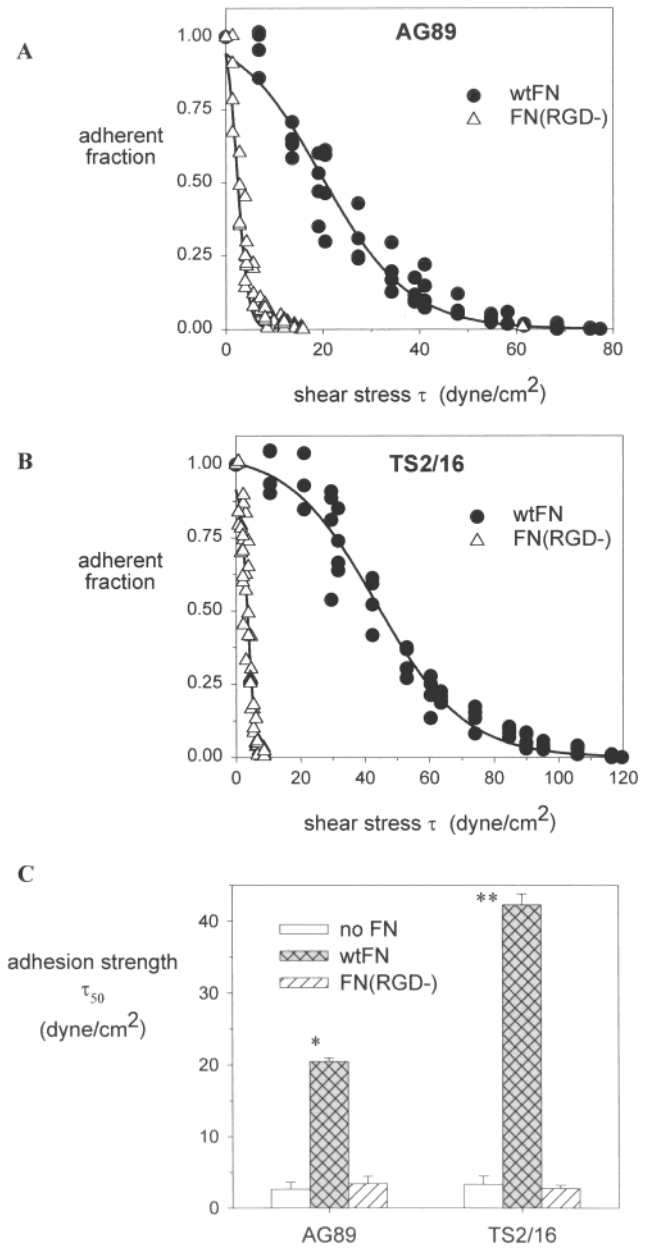

FIGURE 2: K562 adhesion to wtFN and FN(RGD−) for integrins activated with either (A) AG89 or (B) TS2/16. (C) Strength of adhesion of K562 (means ± SEM) to recombinant fibronectins for AG89- and TS2/16-activated α5β1 integrin. Cells were seeded on substrates coated with 5 μg/mL recombinant fibronectins, and adhesion was quantified using the spinning disk device. Deletion of the RGD site completely abolished adhesion for both activation states (one asterisk, $p < 0.01$; two asterisks, $p < 0.0002$).

III repeat of fibronectin. During the time course of the normal process of adhesion to fibronectin, the weaker binding state preceded the stronger binding state (*12*). This reduction in the affinity of α5β1 for RGD as the overall adhesion strength increased was unexpected and suggests that a realignment in the interface between α5β1 and fibronectin takes place in the transition from weaker to stronger mechanical coupling.

Interaction of α5β1-Activated States with the Synergy Domain. The strength of the interaction between TS2/16- and AG89-activated α5β1 with wild-type fibronectin was compared to that of adhesion to the synergy site mutant fibronectin. Figure 4 shows that the AG89-activated form

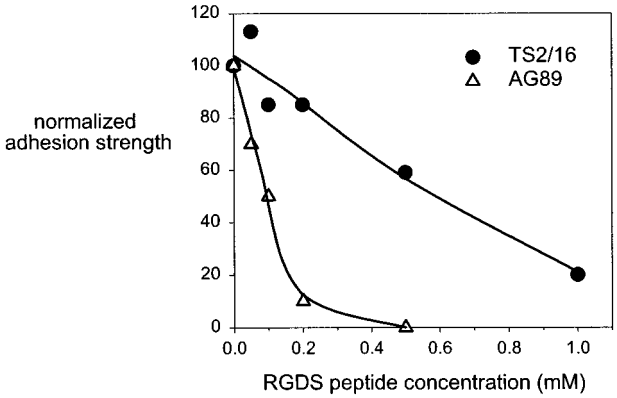

FIGURE 3: Inhibition of α5β1 integrin binding to wtFN by soluble RGDS peptide showing differences in inhibition efficiency between AG89- and TS2/16-activated integrins. K562 cells were seeded on substrates coated with 5 μg/mL wtFN in the presence of varying concentrations of RGDS peptide, and adhesion was quantified at 15 min using the spinning disk device. Normalized adhesion strength values were calculated by dividing the measured adhesion strength by the adhesion strength in the absence of RGDS peptide.

exhibited no significant adhesion to the synergy mutant, whereas the TS2/16-activated form retained approximately 30% of its wild-type adhesion strength, which was 4-fold over the background adhesion levels. This residual adhesion for TS2/16-activated integrins to the synergy mutant could arise from an increase in the binding strength of TS2/16-activated α5β1 to RGD relative to that of the AG89-activated form or through interactions with residues outside both the RGD and synergy sites. This difference cannot be resolved using RGD peptides to block potential interaction with the RGD site because, even though it provides no dectable mechanical strength (see below), the RGD site is essential for all α5β1-mediated adhesion reported here (Figure 2). It is unlikely that the residual adhesion of the TS2/16-activated α5β1 is due to the changes in affinity for RGD since the TS2/16-activated form has reduced rather than increased affinity for RGD (Figure 3) and hence would be expected to have a lower adhesion strength. However, the affinity of different α5β1 forms for RGD was measured by inhibition rather than directly, so it is possible that the affinity of the TS2/16-activated form for soluble RGD was reduced while its affinity for the constrained RGD loop in fibronectin was increased. To test this possibility, a genetically engineered protein containing 13 RGD loops constrained to mimic the RGD motif in fibronectin was used as described below. This protein failed to support any α5β1 coupling, and the simplest interpretation of this result is that the constrained RGD does not show an increased level of interaction with the TS2/16-activated form of α5β1.

These results imply that the TS2/16-activated form of α5β1 binds to sites on fibronectin outside the PHSRN synergy and RGD domains. Mutational analysis of additional sites on the interacting face of the 9th type III repeat demonstrated that TS2/16-activated α5β1 interacts with amino acid residues distributed over this surface (*31*). Thus, the difference in binding strengths for the two activated forms appears to depend on their interactions with different residues of the 9th type III repeat rather than on differences in their interactions with the RGD and synergy domains as originally postulated. Attempts to interfere with the binding of either activated integrin state to fibronectin by the addition of

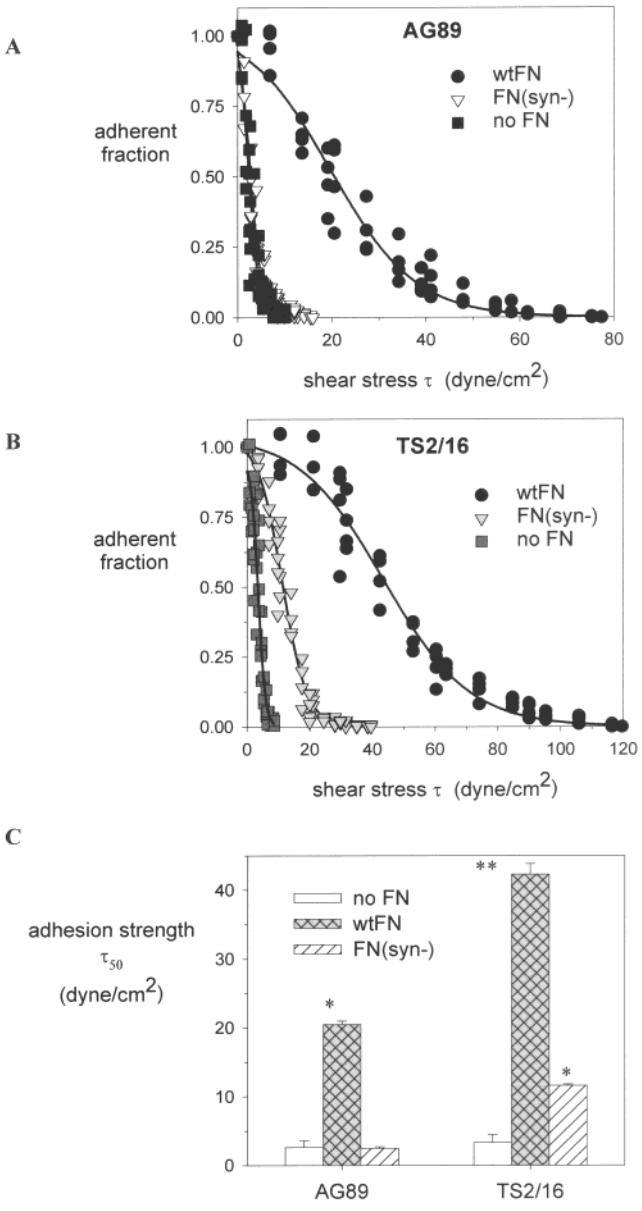

FIGURE 4: K562 adhesion to wtFN and FN(syn−) for integrins activated with either (A) AG89 or (B) TS2/16. (C) Strength of adhesion of K562 (means ± SEM) to recombinant fibronectins for AG89- and TS2/16-activated α5*β*1 integrin. Cells were seeded on substrates coated with 5 *μ*g/mL recombinant fibronectins, and adhesion was quantified using the spinning disk device. Mutation of the synergy site completely inhibited adhesion of AG89-activated α5*β*1 integrin, while TS2/16-activated integrins retained approximately 30% of the strength of adhesion to wild-type fibronectin (one asterisk, $p < 0.01$; two asterisks, $p < 0.0002$).

soluble PHSRN peptide were not successful. This probably results from a low binding affinity of α5*β*1 for this peptide (*22*).

Failure of the RGD Domain To Provide Mechanical Coupling. A surprising result from the previously collected data is the lack of mechanical coupling of AG89-stimulated integrin to RGD in the absence of the synergy site (Figure 4A). A simple explanation for the lack of coupling between activated α5*β*1 and FN(syn−) is that binding of α5*β*1 to RGD in the absence of PHSRN is a low-affinity interaction and does not produce sufficient mechanical coupling due to relatively low numbers of bound receptors. To examine whether high concentrations of the RGD motif provide

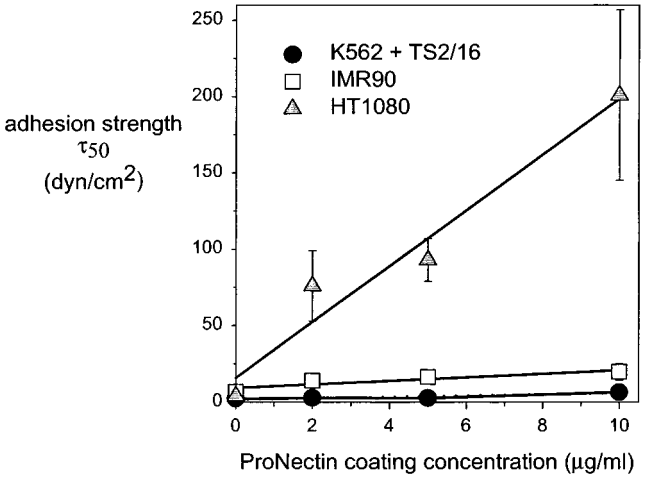

FIGURE 5: Strength of cell adhesion to ProNectin-coated surfaces. Adhesion strength for TS2/16-activated K562 cells and IMR90 fibroblasts was indistinguishable from background. Under the conditions of the assay, these cells only use α5*β*1 to adhere to fibronectin. Linear increases in adhesion strength with ProNectin coating concentration for HT1080 fibroblasts, which also express α*v*β3, demonstrated that the adsorbed ProNectin was active.

mechanical coupling, α5*β*1-mediated adhesion to ProNectin (Protein Polymer Technologies, San Diego, CA) was quantified. ProNectin is an engineered polymer presenting 13 copies of the 10-amino acid RGDS binding loop (VTGRGDSPAS) of fibronectin that supports adhesion of several cell types. For our experimental conditions, we estimate that this polymer provides approximately 50-fold increases in RGD surface density compared to fibronectin. For both AG89- and TS2/16-activated K562 cells and IMR90 fibroblasts [which only use α5*β*1 for binding to fibronectin in the initial 15 min (*12*)], the strength of adhesion to ProNectin was indistinguishable from background adhesion (Figure 5). On the other hand, RGD alone did provide significant mechanical coupling for HT1080 cells, which also use α*v*β3 to attach to fibronectin (Figure 5) (*23*, *34*). On the basis of estimates for binding affinities from competitive inhibition studies with fibronectin fragment mutants in the RGD and PHSRN sites (*22*), we cannot attribute the complete absence of adhesion strength to ProNectin to reduced binding affinity for the RGD site. Taken together, these results suggest that the RGD domain by itself does not contribute significantly to the mechanical coupling of either antibody- or cell-activated α5*β*1. These results underscore the importance of binding to both domains for robust mechanical coupling to the activated receptor.

DISCUSSION

This study employed a novel experimental approach to the analysis of the interaction of α5*β*1 integrin with the PHSRN and RGD domains in the 9th and 10th type III repeats of fibronectin. Using two previously defined monoclonal antibodies to *β*1 integrin which activate α5*β*1 for binding to fibronectin, two activated states of α5*β*1 integrin were produced which can be distinguished on the basis of the strength of the receptor−ligand bond (*12*). During the normal process of adhesion of IMR90 fibroblasts to fibronectin, short-term binding is controlled by the weaker (AG89-activated) state, whereas at later times, the stronger

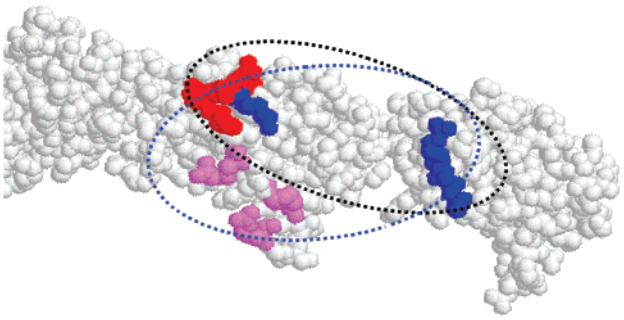

FIGURE 6: Model of the three-dimensional structure of the 9th and 10th type III repeats of fibronectin [PDB entry 1fnf (*44*)] highlighting key residues for α5β1 binding.

(TS2/16-activated) state dominates. Using rat recombinant fibronectins, analysis of the interaction of these two states of α5β1 with fibronectin mutants demonstrated that the transition from the weaker to the stronger state involved a reduction in the binding affinity of α5β1 for RGD and the interaction of α5β1 with new sites in fibronectin which are outside both the RGD and PHSRN domains. These results provide additional support for the model of multiple binding states for α5β1 and focus on the importance of interaction with new sites on fibronectin for the activation process. In addition, measurements of the strength of the α5β1−fibronectin interaction revealed the surprising result that the RGD domain by itself does not contribute significantly to the mechanical coupling of α5β1 to fibronectin. The failure of the RGD loop to provide mechanical coupling was confirmed using ProNectin to increase the density of RGD loops in the absence of synergy-like domains. Interestingly, the RGD motif alone provided robust coupling to integrin αvβ3, suggesting divergent roles for RGD among integrin family members.

What are the differences in binding of the two activated states of α5β1 which explain the differences in the α5β1−fibronectin bond strengths? Figure 6 shows a model of the three-dimensional structure of the 9th and 10th type III repeats of fibronectin highlighting key residues for α5β1 binding. Previous site-directed mutagenesis studies identified R1379 as a critical residue in the PHRSN site (*22*, *31*). In the study presented here, mutation of this arginine eliminated mechanical coupling to AG89-activated α5β1, but reduced the level of mechanical coupling to TS2/16-activated α5β1 by 70%. Using a centrifugation assay, it has been demonstrated that residues R1374, R1369, and R1371 on the interacting face of the 9th type III repeat are involved in the binding of TS2/16-activated α5β1 and hence represent a likely explanation for the residual binding of activated α5β1 observed in the study presented here (*31*). Importantly, this analysis suggests that the α5β1−fibronectin binding interface is different for the two activated forms of the integrin. On the basis of current concepts of protein−protein association (*35*−*37*), these differences in the binding interface probably give rise to the observed functional differences in binding strength. This suggests a novel "gripping" mechanism by which the conformation of the *ligand-bound integrin* is altered to modulate the binding interface and, consequently, receptor−ligand binding strength.

We attribute the functional differences in binding strength to differences in the binding interface arising from distinct conformations of the integrin. Mapping studies implicate the α5 integrin subunit in binding to the synergy domain, while the RGD loop appears to interact with both α5 and β1 subunits (*38*−*41*). Interestingly, the monoclonal activating antibodies used in this study bind to structural epitopes on the β1 subunit. This suggests that antibody-induced conformational changes in the β1 subunit can be propagated to the α5 subunit to modify interactions with the synergy site. Alternatively, structural changes in the β1 subunit could alter the alignment of the receptor relative to the fibronectin to interact with different residues in the 9th type III repeat.

If the RGD loop does not provide significant mechanical coupling, what is its role in α5β1-mediated adhesion to fibronectin? This study supports a central role for RGD in the binding of α5β1 integrin to fibronectin, consistent with a large body of literature. An interesting possibility is that RGD functions to activate or align α5β1 to promote binding to the 9th type III repeat. In fact, previous reports suggest that binding of RGD peptides to α5β1 results in changes in integrin conformation (*42*, *43*). Addition of soluble RGD leads to localization of α5β1 to focal adhesion complexes, probably by inducing changes in integrin conformation that allow interactions with cytoskeletal components. Crystallographic analysis of fibronectin type III repeats 7−10 shows the RGD loop protruding approximately 12 Å above the surface of the 10th type III repeat and at the end nearest to the 9th type III repeat (Figure 6) (*44*). This places the RGD domain in a location that is ideal for providing the initial interaction with α5β1 integrin on a cell surface. Steered molecular dynamic simulations of the 10th type III repeat of fibronectin have demonstrated that application of extensional forces induces retraction of the RGD loop (*45*). This force-generated retraction of the RGD domain could promote binding to the synergy domain since the receptor would be drawn closer to and could be properly oriented relative to the synergy domain. This is consistent with the reduced binding affinity for the more highly activated α5β1 state. Furthermore, the reported flexibility of the RGD loop (*46*, *47*) and the hinge connecting the 9th and 10th type III repeats (*44*, *47*) may be important in the binding interactions with α5β1. Steered molecular simulations of the unfolding of a fragment spanning the 9th and 10th type III repeats of fibronectin revealed an intermediate extensional state in which the distance between the RGD and PHSRN sites is altered (*48*, *49*).

These results suggest a new model for the interaction of fibronectin with α5β1 integrin. The initial interaction with the RGD domain is necessary to activate α5β1 in the proper alignment for interaction with the synergy domain in the 9th type III repeat. This is followed by a conformational change in α5β1 and possibly in fibronectin which reduces the level of binding to RGD and shifts the load-bearing interface to the synergy domain. As the adhesion strength increases, there is a spreading of the interaction to include additional regions of the 9th type III repeat and increase the number of intramolecular contributions to binding strength. The inclusion of regions outside the PHSRN site in the binding of α5β1 to the 9th type III repeat would be consistent with the studies showing that the requirement for PHSRN can be abrogated by activation of the receptor (*7*, *23*). Finally, in addition to differences in the integrin−fibronectin binding interaction, these different integrin activated states may interact differentially with intracellular signaling and cy-

toskeletal components, providing a versatile mechanism for the regulation of adhesive interactions.

ACKNOWLEDGMENT

We thank C. H. Damsky and J. Takagi for providing anti-integrin antibodies and R. O. Hynes for the BR5.4 antibody. We acknowledge Ms. Laura Lynch for technical assistance. We also thank H. P. Erickson and D. F. Mosher for helpful discussion and critical review of the manuscript.

REFERENCES

1. Hynes, R. O. (1992) *Cell 69*, 11−25.
2. Smyth, S. S., Joneckis, C. C., and Parise, L. V. (1993) *Blood 81*, 2827−2843.
3. Albelda, S. M. (1993) *Lab. Invest. 68*, 4−17.
4. Schwartz, M. A., Schaller, M. D., and Ginsberg, M. H. (1995) *Annu. Rev. Cell Dev. Biol. 11*, 549−599.
5. Bennett, J. S., and Vilaire, G. (1979) *J. Clin. Invest. 64*, 1393−1401.
6. Wu, C., Keivens, V. M., O'Toole, T. E., MacDonald, J. A., and Ginsberg, M. H. (1995) *Cell 83*, 715−724.
7. Sechler, J. L., Corbett, S. A., and Schwarzbauer, J. E. (1997) *Mol. Biol. Cell 8*, 2563−2573.
8. Adams, J. C., and Watt, F. M. (1990) *Cell 63*, 425−435.
9. Boettiger, D., Enomoto-Iwamoto, M., Yoon, H. Y., Hofer, U., Chiquet-Ehrismann, R., and Menko, A. S. (1995) *Dev. Biol. 169*, 261−272.
10. Takagi, J., Erickson, H. P., and Springer, T. A. (2001) *Nat. Struct. Biol. 8*, 412−416.
11. Shattil, S. J., Hoxie, J. A., Cunningham, M., and Brass, L. F. (1985) *J. Biol. Chem. 260*, 11107−11114.
12. García, A. J., Takagi, J., and Boettiger, D. (1998) *J. Biol. Chem. 273*, 34710−34715.
13. Sims, P. J., Ginsberg, M. H., Plow, E. F., and Shattil, S. J. (1991) *J. Biol. Chem. 266*, 7345−7352.
14. Fenczik, C. A., Sethi, T., Ramos, J. W., Hughes, P. E., and Ginsberg, M. H. (1997) *Nature 390*, 81−85.
15. Zhang, Z., Vuori, K., Wang, H., Reed, J. C., and Ruoslahti, E. (1996) *Cell 85*, 61−69.
16. Hughes, P. E., Renshaw, M. W., Pfaff, M., Forsyth, J., Keivens, V. M., Schwartz, M. A., and Ginsberg, M. H. (1997) *Cell 88*, 521−530.
17. Gailit, J., and Ruoslahti, E. (1988) *J. Biol. Chem. 263*, 12927−12932.
18. Frelinger, A. L., Du, X. P., Plow, E. F., and Ginsberg, M. H. (1991) *J. Biol. Chem. 266*, 17106−17111.
19. van de Wiel-Kemenade, E., van Kooyk, Y., de Boer, A. J., Huijbens, R. J. F., Weber, P., van de Kasteele, W., Melief, C. J. M., and Figdor, C. G. (1992) *J. Cell Biol. 117*, 461−470.
20. Mould, A. P., Akiyama, S. K., and Humphries, M. J. (1995) *J. Biol. Chem. 270*, 26270−26277.
21. Pierschbacher, M. D., Hayman, E. G., and Ruoslahti, E. (1983) *Proc. Natl. Acad. Sci. U.S.A. 80*, 1224−1227.
22. Aota, S., Nomizu, M., and Yamada, K. M. (1994) *J. Biol. Chem. 269*, 24756−24761.
23. Danen, E. H., Aota, S., van Kraats, A. A., Yamada, K. M., Ruiter, D. J., and van Muijen, G. N. (1995) *J. Biol. Chem. 270*, 21612−21618.
24. Miyamoto, S., Teramoto, H., Coso, O. A., Gutkind, J. S., Burbelo, P. D., Akiyama, S. K., and Yamada, K. M. (1995) *J. Cell Biol. 131*, 791−805.
25. García, A. J., Vega, M. D., and Boettiger, D. (1999) *Mol. Biol. Cell 10*, 785−798.
26. Sechler, J. L., Takada, Y., and Schwarzbauer, J. E. (1996) *J. Cell Biol. 134*, 573−583.
27. García, A. J., Huber, F., and Boettiger, D. (1998) *J. Biol. Chem. 273*, 10988−10993.
28. Hemler, M. E., Huang, C., and Schwarz, L. (1987) *J. Biol. Chem. 262*, 3300−3309.
29. Faull, R. J., Kovach, N. L., Harlan, J., and Ginsberg, M. H. (1993) *J. Cell Biol. 121*, 155−162.
30. Obara, M., Kang, M. S., and Yamada, K. M. (1988) *Cell 53* (4), 649−657.
31. Redick, S. D., Settles, D. L., Briscoe, G., and Erickson, H. P. (2000) *J. Cell Biol. 149*, 521−527.
32. Boettiger, D., Huber, F., Lynch, L., and Blystone, S. (2001) *Mol. Biol. Cell 12*, 1227−1237.
33. Chi-Rosso, G., Gotwals, P. J., Yang, J., Ling, L., Jiang, K., Chao, B., Baker, D. P., Burkly, L. C., Fawell, S. E., and Koteliansky, V. E. (1997) *J. Biol. Chem. 272*, 31447−31452.
34. Bowditch, R. D., Hariharan, M., Tominna, E. F., Smith, J. W., Yamada, K. M., Getzoff, E. D., and Ginsberg, M. H. (1994) *J. Biol. Chem. 269*, 10856−10863.
35. Chothia, C., and Jain, J. (1975) *Nature 256*, 705−708.
36. Clackson, T., and Wells, J. A. (1995) *Science 267*, 383−386.
37. Cunningham, B. C., and Wells, J. A. (1993) *J. Mol. Biol. 234*, 554−563.
38. Baneres, J. L., Roquet, F., Green, M., LeCalvez, H., and Parello, J. (1998) *J. Biol. Chem. 273*, 24744−24753.
39. Baneres, J. L., Roquet, F., Martin, A., and Parello, J. (2000) *J. Biol. Chem. 275*, 5888−5903.
40. Humphries, J. D., Askari, J. A., Zhang, X. P., Takada, Y., Humphries, M. J., and Mould, A. P. (2000) *J. Biol. Chem. 275*, 20337−20345.
41. Mould, A. P., Askari, J. A., and Humphries, M. J. (2000) *J. Biol. Chem. 275*, 20324−20336.
42. LaFlamme, S. E., Akiyama, S. K., and Yamada, K. M. (1992) *J. Cell Biol. 117*, 437−447.
43. Miyamoto, S., Akiyama, S. K., and Yamada, K. M. (1995) *Science 267*, 883−885.
44. Leahy, D. J., Aukhil, I., and Erickson, H. P. (1996) *Cell 84*, 155−164.
45. Krammer, A., Lu, H., Isralewitz, B., Schulten, K., and Vogel, V. (1999) *Proc. Natl. Acad. Sci. U.S.A. 96*, 1351−1356.
46. Main, A. L., Harvey, T. S., Baron, M., Boyd, J., and Campbell, I. D. (1992) *Cell 71*, 671−678.
47. Copie, V., Tomita, Y., Akiyama, S. K., Aota, S., Yamada, K. M., Venable, R. M., Pastor, R. W., Krueger, S., and Torchia, D. A. (1998) *J. Mol. Biol. 277*, 663−682.
48. Craig, D., Krammer, A., Schulten, K., and Vogel, V. (2001) *Proc. Natl. Acad. Sci. U.S.A. 98*, 5590−5595.
49. Vogel, V., Thomas, W. E., Craig, D. W., Krammer, A., and Baneyx, G. (2001) *Trends Biotechnol. 19*, 416−423.

BI025752F